

Primordial gravitational waves spectrum in the interacting Bose-Einstein gas model

Germán Izquierdo,¹ Gildardo Alonzo,¹ and Jaime Besprosvany²

¹*Facultad de Ciencias, Universidad Autónoma del Estado de México,
Toluca 5000, Instituto literario 100, Estado de México, México **

²*Instituto de Física, Universidad Nacional Autónoma de México,
Apartado Postal 20-364, Ciudad de México 01000, México*

(Dated: February 16, 2022)

Abstract

We study the evolution and power spectrum of primordial gravitational waves in the interactive Bose-Einstein gas model for dark energy, relevant, as it addresses the coincidence problem. The model is applied in the radiation, matter and dark-energy domination stages. The model introduces a scale factor associated to the radiation-matter transition which influences the gravitational spectrum. We focus on the impact of the free parameters on both the gravitational waves amplitude and its power-spectrum slope. For sets of parameters fitting Hubble's law, we show that the model's parameter for today's dark-matter energy density has a noticeable impact on such waves, while the others produce an indistinguishable effect. The feasibility of detecting such waves under present and future measurements is discussed.

*Electronic address: gizquierdos@uaemex.mx

I. INTRODUCTION

Gravitational waves (GW) are second-order tensorial propagating wave-like solutions to General Relativity's field equations that were predicted by Einstein back in 1916 [1]. GW are generated by different kinds of sources (pulsars, merging Black Holes, the Big Bang) and their evolution equations can be obtained by considering them as a perturbation of a corresponding background metric. Indirect observation of the GW through the period variation of the binary pulsar PSR1913+16 was obtained in 1975 [2]. More recently, LIGO and VIRGO succeeded in observing GW directly [3].

Cosmology can take advantage of the GW physics in different ways. Astrophysical events that emit GW as well as electromagnetic radiation can be used to estimate the Universe expansion rate (Hubble constant) [4, 5]. This estimation is particularly useful to solve the problem of the Hubble-constant tension between its measurements made by the PLANCK Project [6] and by the Hubble Space Telescope (HST) [7]. Primordial Gravitational Waves (PGW) are perturbations of the Friedman-Lemaitre-Robertson-Walker metric whose amplitude evolves during the universe expansion in a characteristic way [8, 9]. PGW have a small energy density on the ground-based detector frequencies which make very difficult the direct detection. In fact, the PGW power spectrum can be bounded by the Laser Interferometer Gravitational-Wave Observatory (LIGO) experiment [10]. Future space-based detectors like eLISA, the Laser Interferometer Space Antenna, [11] could change this scenario and open the window to direct detection. Also, B-mode polarization on the Cosmic Microwave Background radiation is generated by low-frequency PGW present at the last-scattering surface [12]. It would be possible to reconstruct or at least to put bounds on the PGW spectrum through this kind of observed data [13].

The Universe is experiencing a late-stage accelerated expansion [6] induced by an unknown energy-density source called Dark Energy (DE). Although the cosmological constant model is the most favoured by observational data [6], it is plausible to consider other DE models [14]. In particular, coupled DE models describe a dark-sector interaction (i.e. DE interacts with cold dark matter through a coupling term) [15], addressing the coincidence problem.

Exchange models are constructed based on physical processes. In a class of model-dependence on the number-density and energy-density components, for the IBEG model

term, it emerges from a fluid decay process common in astrophysical processes [16]; other models rely on the dependence on the energy-density components' time derivative [17], with a description of stable fixed points. In these models, attractor solutions solve the coincidence problem. Dark-energy evolution can also be ascribed to a time dependence of the cosmological component [18], as such a model emerges from scalar-field models at the inflationary time [19, 20]

While the early-expansion model (inflation and phase transitions) is fundamental to the PGW amplitude evolution, the late stage has also an important impact on the low-frequency wave amplitude and power spectrum [21]. In [22], the authors find an exact solution for PGW in a universe with a cosmological constant. In [23], some coupled DE models are considered as well, describing the amplitude and power spectrum of the PGW in terms of the model's free parameters.

The Interacting Bose-Einstein Gas (IBEG) model assumes the DE is a gas of non-relativistic Bose-Einstein self-interacting particles; for the late-expansion description it couples to cold dark matter (CDM) in a way that the IBEG particle number changes with the expansion [24, 25]. The IBEG model has a detailed microscopic description and the model's free parameters can be bounded by observational data [26]. In this work, we study the evolution and power spectrum of PGW in the IBEG model. We focus on the impact of the free-parameter choices on both the PGW amplitude and its power-spectrum slope. We demonstrate how the choice of the parameter Ω_{m0} , related to CDM mass density energy, has a noticeable impact on the PGW, while the rest of the parameters lead to a similar amplitude and power spectrum. Obtaining observational data of the low-frequency PGW power spectrum could help bound parameter Ω_{m0} of the IBEG model.

The plan of the article is as follows: In section II, we briefly review the PGW amplitude evolution equations. In section III, we address the IBEG universe dynamics and compute PGW amplitudes for different free-parameter choices. In section IV, we estimate the power spectrum of the PGW. Finally, in section V, we summarize the findings.

We assume units for which $c = \hbar = k_B = 1$. As usual, a zero subindex refers to the current value of the corresponding quantity; likewise, we normalize the scale factor of the metric by setting $a_0 = 1$.

II. PGW EVOLUTION FROM THE BIG BANG UNTIL THE RADIATION ERA

We define $h_{\alpha\beta}$ as perturbations of the background Lemaitre-Friedman-Robertson-Walker (LFRW) metric. The total metric reads $\bar{g}_{\alpha\beta} = g_{\alpha\beta} + h_{\alpha\beta}$, $|h_{\alpha\beta}| \ll |g_{\alpha\beta}|$, $\alpha, \beta = 0, 1, 2, 3$. The background $g_{\alpha\beta}$ is the flat homogeneous and isotropic LFRW metric

$$ds^2 = -dt^2 + a(t)^2 [dr^2 + r^2 d\Omega^2] = a(\eta)^2 [-d\eta^2 + dr^2 + r^2 d\Omega^2],$$

where t and η are, respectively, the cosmic and conformal time ($a(\eta)d\eta = dt$), with comoving coordinates, r , the radius, and Ω , the solid angle.

To obtain the sourceless perturbation evolution to linear order (PGW), we choose the transverse-traceless tensor gauge. The resulting equations can be expressed as [8, 9]

$$\begin{aligned} h_{ij}(\eta, \mathbf{x}) &= \int h_{ij}^{(\mathbf{k})}(\eta, \mathbf{x}) d^3k, \\ h_{ij}^{(\mathbf{k})}(\eta, \mathbf{x}) &= \frac{\mu(\eta)}{a(\eta)} G_{ij}(\mathbf{k}, \mathbf{x}), \end{aligned} \quad (1)$$

where space indices use latin letters and run from 1 to 3, \mathbf{x} is the comoving Cartesian coordinate, and \mathbf{k} is the comoving wave vector. The functions $G_{ij}(\mathbf{k}, \mathbf{x})$ satisfy the equations

$$G_{i;m}^{j;m} = -k^2 G_i^j, \quad G_{i;j}^j = G_i^i = 0, \quad (2)$$

implying for $\mu(\eta)$

$$\mu''(\eta) + \left[k^2 - \frac{a''(\eta)}{a(\eta)} \right] \mu(\eta) = 0, \quad (3)$$

where the prime indicates derivative with respect to the conformal time, and $k = |\mathbf{k}|$ is the constant wave number, related to the physical wavelength and frequency by $k = 2\pi a/\lambda = 2\pi a f = a \omega$. The functions G_i^j are combinations of $\exp(\pm i\mathbf{k} \cdot \mathbf{x})$, which contain the two possible wave polarizations, compatible with the conditions (2).

Eq. (3) is a time-independent Schrödinger equation with potential term a''/a . When $k^2 \gg \frac{a''}{a}$, i.e., for waves whose wavelength is smaller than the horizon, expression (3) becomes a free-wave equation. The $h_{ij}^{(\mathbf{k})}(\eta, \mathbf{x})$ amplitude tends to null adiabatically as a^{-1} in an expanding universe. In the opposite regime, when $k^2 \ll \frac{a''}{a}$, i.e., when the PGW wavelength is larger than the horizon, the solution to (3) is a lineal combination of $\mu_1 \propto a(\eta)$ and $\mu_2 \propto a(\eta) \int d\eta a^{-2}$. In an expanding universe, μ_1 grows faster than μ_2 and will soon

dominate. The $h_{ij}^{(\mathbf{k})}(\eta, \mathbf{x})$ amplitude is constant while the condition $k^2 \ll \frac{a''}{a}$ is fulfilled. When the PGW reenter the horizon, the wave will have an amplitude greater than it would in the adiabatic behavior. This phenomenon is known as “superadiabatic amplification” of PGW [9, 27].

For sources with constant equation of state, the resulting scale factor is a power-law expansion $a \propto \eta^l$ ($l = -1, 1, 2$ for de Sitter, radiation dominated and dust-dominated universes, respectively). Equation (3) is a Bessel equation with solution

$$\mu(\eta) = (k\eta)^{\frac{1}{2}} \left[C_1 J_{l-\frac{1}{2}}(k\eta) + C_2 J_{-(l-\frac{1}{2})}(k\eta) \right],$$

where $J_{l-\frac{1}{2}}(k\eta)$, $J_{-(l-\frac{1}{2})}(k\eta)$ are Bessel functions of the first kind and $C_{1,2}$ are integration constants.

We assume now that the early universe experiences an inflationary de Sitter stage of evolution, followed by a radiation-dominated stage, and a dust stage [27]. Transitions between successive eras are assumed instantaneous. This approach is known as the sudden transition approximation, which is reasonable when the transition time span between the different stages is much lower than the period of the PGW considered. The scale factor, then, is

$$a(\eta) = \begin{cases} -\frac{1}{H_1\eta} & -\infty < \eta < \eta_1 < 0, \\ \frac{1}{H_1\eta_1^2}(\eta - 2\eta_1) & \eta_1 < \eta < \eta_2, \\ \frac{1}{4H_1\eta_1^2} \frac{(\eta + \eta_2 - 4\eta_1)^2}{\eta_2 - 2\eta_1} & \eta_2 < \eta, \end{cases} \quad (4)$$

where the subindexes 1, 2 correspond to the sudden transitions from the inflation to the radiation era and from the radiation to the dust era, respectively, and H_1 represents the Hubble factor at the end of the inflationary era. The solution to eq. (3) for each era is

$$\mu_I(\eta) = C_I \left[\cos(k\eta + \phi_I) - \frac{1}{k\eta} \sin(k\eta + \phi_I) \right] \quad (\text{inflationary era}) \quad (5)$$

$$\mu_R(\eta) = C_R \sin(k\eta_R + \phi_r) \quad (\text{radiation era}) \quad (6)$$

$$\mu_D(\eta) = C_D \left[\cos(k\eta_D + \phi_D) - \frac{1}{k\eta_D} \sin(k\eta_D + \phi_D) \right] \quad (\text{dust era}), \quad (7)$$

where $C_{I,R,D}$, $\phi_{I,R,D}$ are integration constants, $\eta_R = \eta - 2\eta_1$ and $\eta_D = \eta + \eta_2 - 4\eta_1$.

It is possible to express C_R , ϕ_R and C_D , ϕ_D in terms of C_I , ϕ_I as $\mu(\eta)$ must be continuous at the transition times $\eta = \eta_1$ and $\eta = \eta_2$. Averaging the solution over the initial phase ϕ_I , the amplification factor is

$$\frac{C_D}{C_I} \sim \begin{cases} 1 & k \gg -1/\eta_1, \\ k^{-2} & -1/\eta_1 \gg k \gg 1/\eta_{D2}, \\ k^{-3} & 1/\eta_{D2} \gg k, \end{cases} \quad (8)$$

where $\eta_{D2} = 2\eta_2 - 4\eta_1$.

The PGW evolution from the dust era up to the present day depends on the late-acceleration stage considered. As the universe experiences such a stage, the potential term a''/a becomes an increasing function of η . Consequently, some waves that were already in the $k^2 \gg a''/a$ regime reenter the $k^2 \ll a''/a$ regime, and cease contributing to the PGW physical power spectrum. In [21], the amplification is computed for different constant equations of state in dark-energy models. In [23], two coupled dark-energy scenarios are considered. In [22], an exact solution to the late acceleration ruled by the cosmological constant is found. In all cases, it is important that the late-stage acceleration universe leaves a characteristic amplification on low-frequency waves.

In the next section, we consider a different scenario in which a coupled IBEG stage follows the radiation era.

III. PGW EVOLUTION FROM THE RADIATION ERA UP TO PRESENT TIME

A. IBEG model and expansion factor

The IBEG model for the late-acceleration stage assumes the universe has three energy-density sources: baryonic matter ρ_b , cold dark matter (CDM) ρ_{dm} and the IBEG ρ_g [25, 26]. The latter is a gas of Bose-Einstein particles that self-interact attractively with non-null kinetic energy. An energy flux is imposed between the IBEG and the CDM, which induces the non-condensate IBEG particle number density to evolve as $n_\epsilon = n_{\epsilon 0} a^{3(x-1)}$, where $n_{\epsilon 0}$ is the IBEG number density today, and x is the parameter that models the Markoff variation process of the IBEG particles[31]. In [25], the parameter x is found to be in the range $0.85 \leq x \leq 1$. On one hand, $x \geq 1$ would lead to an IBEG number density increasing with expansion, which eventually would make the IBEG energy density negative as well, while for $x < 0.85$, the IBEG model does not solve the coincidence problem. The gas energy density

and pressure evolve with the expansion as [25]

$$\rho_g = \rho_{G0}a^{3(x-1)} + \rho_{c0}a^{5(x-1)} + \rho_{i0}a^{6(x-1)}, \quad (9)$$

$$p_g = \frac{2}{3}\rho_{c0}a^{5(x-1)} + \rho_{i0}a^{6(x-1)}, \quad (10)$$

where ρ_{G0} is the model's free parameter connected the IBEG particles' mass, ρ_{c0} relates to the IBEG kinetic energy, and ρ_{i0} is the self-interaction term ($\rho_{i0} < 0$).

As our IBEG model relies on an attractive self-interaction, we address the model's gas stability. In [28], the gravitational stability of a scalar field is studied with a repulsive/attractive self-interaction $\mp\lambda^2\phi^4$ in the Newtonian approximation. The authors find that the Jeans instability is similar to that of a dust model with extra 'hydrodynamic' self-interaction effects. In particular, for the attractive case ($+\lambda^2\phi^4$), the obtained Jeans wave number is larger than that of the corresponding free scalar field. In the IBEG case, we model a phenomenological short-range two-particle attractive potential through a contact interaction [24, 25], so naturally, $+\lambda^2\phi^4$ is a valid quantum description in the low-density limit. We conclude that the IBEG instabilities would evolve in a similar way to instabilities in [28]. Also, in [25], the linear density-perturbation evolution and corresponding equations were obtained in the cosmological expanding background for both the coupled IBEG gas and the CDM, taking into account the coupling term.

In [19, 20], a Bose condensate models the early-universe accelerated expansion. The Higgs field considered self-interacts through the potential $V(\phi) = \frac{\lambda}{4}(\phi^2 - \phi_0^2)^2$. Such an interaction naturally accounts for slow-roll inflation as well as for the reheating process, as real particles are created by the Higgs particles' decay. In [24], a non-coupled IBEG gas containing both condensate and non-condensate particles is considered in an early universe approach, solving the horizon problem with a super-exponential expansion for some parameter choices. Such a growth allows for density-fluctuation propagation for a large range of scales, suggesting that they are scale invariant, and that primordial fluctuations can be generated.

Addressing the coincidence problem for the universe late-expansion description, some models include coupling between CDM and Bose-Einstein particles. In [18], the Bose-Einstein condensate constitutes a time-varying Λ term while the condensate decay (with the same mechanism described in [19, 20]) produces a coupling proportional to $\dot{\Lambda}$. This approach has differences with the IBEG model. For the latter model, it is the CDM that decays on the IBEG particles (for most parameters), while for the model in [18], the opposite

is the case. In addition, we investigated the case in which the Bose-Einstein particles are created in a non-condensate state, as we concentrate on the non-null kinetic-energy term.

The energy density evolution equations for the IBEG model read

$$\begin{aligned}\dot{\rho}_b + 3H\rho_b &= 0, \\ \dot{\rho}_{dm} + 3H\rho_{dm} &= -Q, \\ \dot{\rho}_g + 3H(\rho_g + p_g) &= Q,\end{aligned}\tag{11}$$

where $H = \dot{a}/a$ is the Hubble expansion factor and Q is the coupling term. From eqs. (9-10) and the above equations, one obtains the coupling term

$$Q = 3Hx \left(\rho_{G0} a^{3x-3} + \frac{5}{3} \rho_{c0} a^{5x-5} + 2\rho_{i0} a^{6x-6} \right).\tag{12}$$

Some coupling terms in the literature are proportional to the Hubble factor H from dimensional analysis considerations, since H is the characteristic time-inverse FLRW quantity [15]. Other coupled models assume heuristically that Q is proportional to the DE and/or CDM energy-density time derivatives, not directly depending on the Hubble factor [17]. In our model, the coupling (12) is proportional to the Hubble factor, which derives from the dependence of n_ϵ on the scale factor and the IBEG microscopic description.

The CDM energy density is solved as

$$\rho_{dm} = \rho_{m0} a^{-3} - \rho_{G0} a^{3(x-1)} + \frac{5x\rho_{c0}}{2-5x} a^{5(x-1)} + \frac{2x\rho_{i0}}{1-2x} a^{6(x-1)},\tag{13}$$

where ρ_{m0} is an integration constant representing the CDM energy density due to its mass today.

Given that the baryonic matter evolves as $\rho_b = \rho_{b0} a^{-3}$ (ρ_{b0} is the baryonic-matter energy density today), the Hubble factor satisfies [26]

$$H^2 = \frac{8\pi G}{3}(\rho_b + \rho_{dm} + \rho_g) = H_0^2 \left[(\Omega_{b0} + \Omega_{m0}) a^{-3} + \frac{2\Omega_{c0}}{2-5x} a^{5(x-1)} + \frac{\Omega_{i0}}{1-2x} a^{6(x-1)} \right],\tag{14}$$

where $\Omega_{a0} = 8\pi G\rho_{a0}/(3H_0^2)$ with $a = b, m, c, i$, and H_0 is the present-day Hubble expansion rate. The present day DM energy density is defined from (13) as

$$\Omega_{dm0} = \Omega_{m0} - \Omega_{G0} + \frac{5x\Omega_{c0}}{2-5x} + \frac{2x\Omega_{i0}}{1-2x}.\tag{15}$$

We observe that Ω_{m0} is not the present-day energy density of DM, but only the term that evolves as a^{-3} ; aside from it, Ω_{dm0} depends the other parameters Ω_{i0} , Ω_{G0} , x related to the coupling between DM and IBEG particles.

The IBEG-model free parameters are H_0 , Ω_{m0} , Ω_{i0} , Ω_{b0} , x and Ω_{G0} , the latter not appearing in the Hubble factor. Ω_{c0} is related to these parameters, as we assume a flat LFRW metric

$$\Omega_{c0} = \frac{2 - 5x}{2} \left(1 - \Omega_{b0} - \Omega_{m0} - \frac{\Omega_{i0}}{1 - 2x} \right). \quad (16)$$

Given the IBEG microscopic description with parameter $\Omega_{i0} < 0$ evolving with the scale factor as $a^{6(x-1)}$, the IBEG energy density ρ_g would tend in the past to negative values when $x \neq 1$ [25]. We can avoid this problem by assuming the flux of energy from CDM to IBEG is an ongoing process that starts no sooner than the instant for which $\rho_g = 0$. We consider then the scale factor a_{in} defined as the solution to

$$\rho_g(a_{in}) = \rho_{G0} a_{in}^{3(x-1)} + \rho_{c0} a_{in}^{5(x-1)} + \rho_{i0} a_{in}^{6(x-1)} = 0, \quad (17)$$

for a given free-parameter set, as the instant at which the creation of IBEG particles starts. The scale factor a_{in} , on its own, is not a new parameter of the model but it is dependent on the free parameters considered. The creation process starting at a_{in} represents a natural solution under the assumptions made for the gas (both the microscopic description of the gas and the particle creation rate) [25]. The coupling between CDM and IBEG particles is common in astrophysical processes[16], giving support to the interaction between particles that leads to the creation rate assumed and that starts at a_{in} . On the other hand, for $x = 1$, ρ_g is constant and does not tend to null at early stages of evolution. In this case, there is no need to consider a_{in} .

The left panel of figure 1 shows the evolution of $\Omega_{dm} = 3\rho_m/(8\pi GH^2)$, $\Omega_g = 3\rho_g/(8\pi GH^2)$ and $\Omega_b = 3\rho_m/(8\pi GH^2)$ vs. scale factor a for different choices of the free parameters. The right panel of figure 1 shows the evolution of effective adiabatic parameter for both CDM ($w_{eff}^{(m)} = Q/\rho_m$) and the effective adiabatic parameter of the IBEG fluid ($w_{eff}^{(g)} = (p_g - Q)/\rho_g$) vs. scale factor a for different choices of free parameters. The effective adiabatic parameter is often considered in coupled dark-energy models and can be defined from the energy by moving the coupling term to the left-hand side of the corresponding conservation equation.

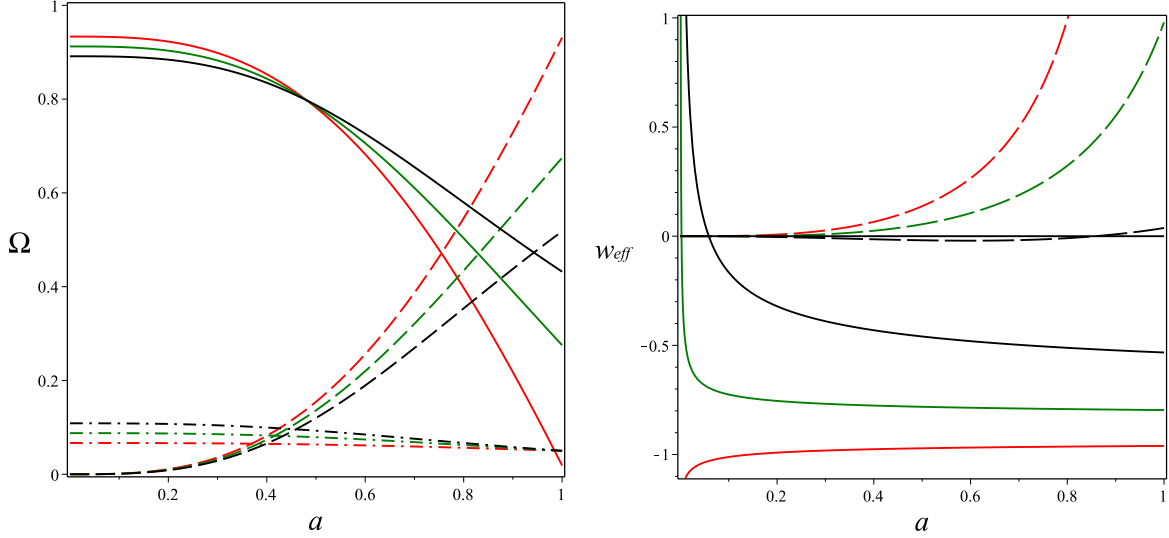


FIG. 1: Left panel: Evolution of Ω_{dm} (solid lines), Ω_g (dashed lines) and Ω_b (dot-dashed lines) vs. scale factor a for $x = 0.97$, $\Omega_{b0} = 0.05$, $\Omega_{i0} = -1.1$, $\Omega_{G0} = 0.72$ and three choices of parameter Ω_{m0} : 0.4 (black lines), 0.52 (green lines), and 0.7 (red lines). Right panel: Evolution of effective adiabatic parameters $w_{eff}^{(g)}$ (solid lines) and $w_{eff}^{(m)}$ (dashed lines) vs. the scale factor a for the same choice of parameters as in the left panel.

In Ref. [26], the expansion rate in eq. (14) is used to adjust the free parameters to three independent sets of Hubble-factor observational data. The best-fit values for the free parameters obtained with the corresponding 1σ likelihood are $H_0 = 70 \pm 2$ km/(Mpsc/s), $\Omega_{m0} = 0.52 \pm 0.08$, $\Omega_{i0} = -3.60 \pm 12.38$, $\Omega_{b0}H_0^2 = 0.022 \pm 0.001$ and $x = 0.97 \pm 0.01$. The results are shown in figure 2, together with two additional theoretical bounds. The first one emerges from the CDM particle mass and IBEG component, which is positive definite

$$\Omega_{dm0} + \Omega_{G0} = \frac{5x}{2} - \frac{5x}{2}\Omega_{b0} + \frac{2-5x}{2}\Omega_{m0} - \frac{x}{2(1-2x)}\Omega_{i0} \geq 0. \quad (18)$$

This bound is represented by the lines on the figure's lhs for different x . The second bound is $\Omega_{c0} > 0$, represented by the lines on the plot's rhs.

Although parameter Ω_{G0} cannot be bounded by observational data on the Hubble factor, it is related to a_{in} , and to the coincidence problem inherent to the IBEG model when $a_{in} \sim 1$ [26]. Given the observational and theoretical bounds on the rest of the parameters (specially x , which is found to be close to unity), no fine tuning on Ω_{G0} is needed to avoid $a_{in} \sim 1$. On the contrary, only a small range of values Ω_{G0} close to zero leads to $a_{in} \sim 1$.

The IBEG-model parameter Ω_{m0} should not be compared with the Λ CDM-model DM parameter, as Ω_{m0} is only a fraction of the DM energy density Ω_{dm0} while other components have a negative contribution due to the coupling term; as Ω_{G0} cannot be bounded by the observational data, we neither can give observational bounds on Ω_{dm0} in the IBEG model, which makes it useless to compare it with the Λ CDM model.

B. PGW late evolution and numerical results

The PGW amplitude, $\mu(\eta)$, evolves with conformal time according to eq. (3). The FLRW universe dynamics affects the amplitude evolution through the potential term a''/a , which relates to the Hubble-factor variable as $ad\eta = dt = da/(Ha)$. The potential a''/a can be expressed in terms of a as

$$\frac{a''(a)}{a} = 2a^2H^2(a) + a^3H(a)\frac{dH(a)}{da}, \quad (19)$$

while eq. (3) is transformed to

$$a^4H^2(a)\frac{d^2\mu(a)}{da^2} + \left[2a^3H^2(a) + a^4H(a)\frac{dH(a)}{da}\right]\frac{d\mu(a)}{da} + \left[k^2 - 2a^2H^2(a) + a^3H(a)\frac{dH(a)}{da}\right]\mu(a) = 0. \quad (20)$$

We note that while integrating eq. (3) in terms of the conformal time η , a''/a is the only term present, as an additional term proportional to $d\mu/da$ appears when integrating in terms of a . For the late-evolution IBEG model, and Hubble factor $H(a)$ given in eq. 14, we can compute $dH(a)/da$, and eventually solve equation (3) by numerical methods for different free-parameter sets.

We consider the free-parameter set of Ω_{m0} , Ω_{i0} , Ω_{G0} , and x , while we fix $\Omega_{b0}H_0^2 = 0.022 (\text{km s}^{-1} \text{Mpc}^{-1})^2$ in order to compute the instant for which the creation process starts $a = a_{in}$. It is possible to divide eq. (20) by H_0^2 and to set $H_0 = 1$ at this point, defining the scale of frequencies of the PGW through wave number k . We set $a_2 = .0001$ as the beginning of the dust era. If $a_{in} \leq 0.0001$, we use the Hubble factor as eq. (14) for $a \in [0.0001, 1]$ in order to solve numerically eq. (20) for different k choices. We use initial conditions at instant $a = 0.0001$ as $\mu(a = 0.0001) = \mu_R(a = 0.0001)$ and $\frac{d\mu}{da}(a = 0.0001) = \frac{d\mu_R}{da}(a = 0.0001)$.

On the other hand, if $a_{in} > 0.0001$, we first solve eq. (20) with the Hubble expansion rate dominated by non-relativistic matter (a mixture of baryonic matter and CDM) as $H(a) =$

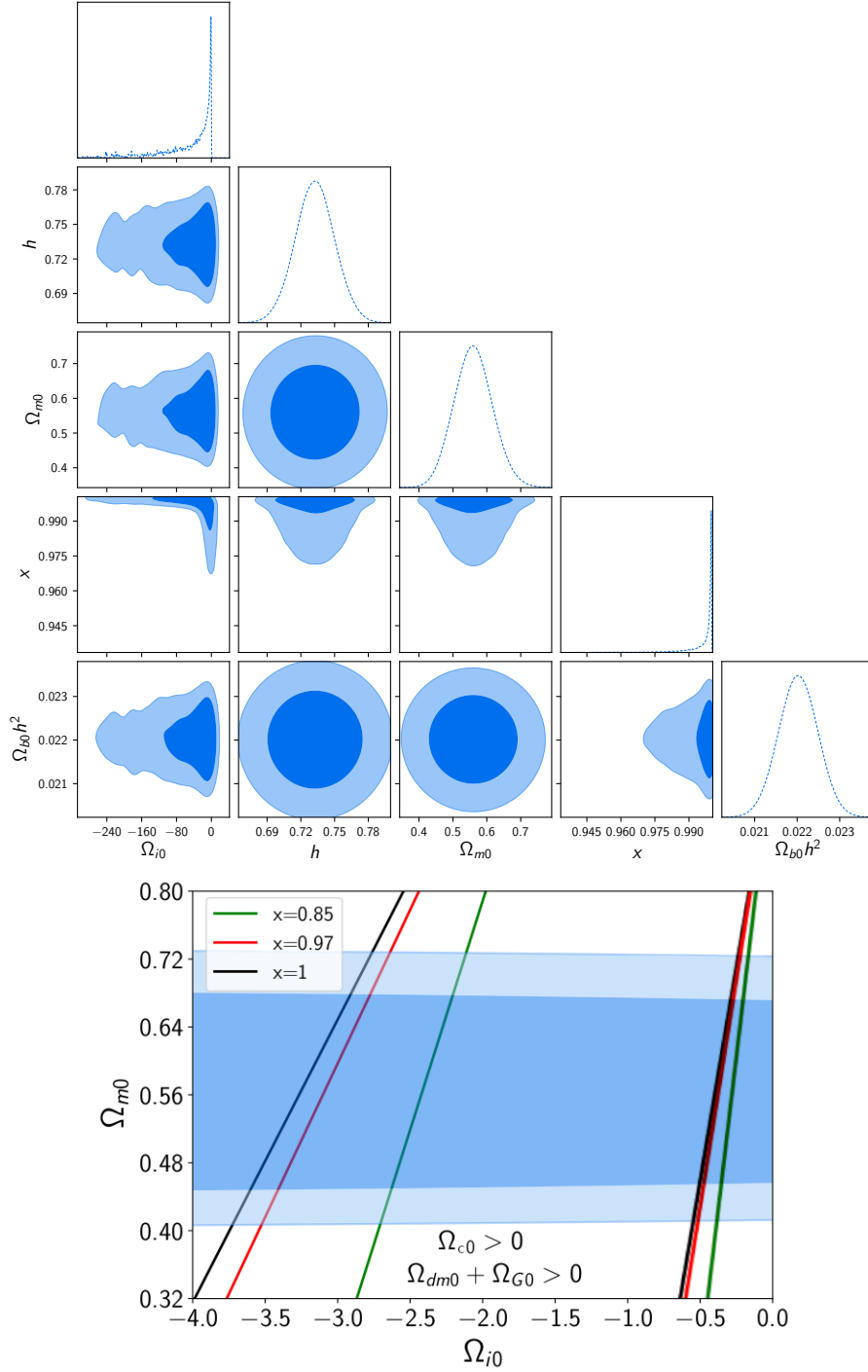


FIG. 2: Top panel: The 1σ and 2σ likelihoods for the free parameters as obtained in [26]. Bottom panel: The 1σ and 2σ likelihoods for the free parameters in the Ω_{m0} vs Ω_{i0} space for $\Omega_{b0}H_0^2 = 0.022$, $H_0 = 70$ km/(Mpc s) shown as obtained in [26]. Lines on the left side of the plot represent the bound $\Omega_{dm0} + \Omega_{G0} = 0$ given by (18) for three different choices of x : $x = 0.85$ (green line), $x = 0.97$ (red line), and, $x = 1$ (black line). Lines on the right side represent the bound $\Omega_{c0} = 0$. The space closed by the lines represents the parameter choices with $\Omega_{dm0} + \Omega_{G0} > 0$ and $\Omega_{c0} > 0$.

$H_{in}(a_{in}/a)^{3/2}$ (where H_{in} is the Hubble factor in eq. (14) evaluated at scale factor a_{in}) for $a \in [0.0001, a_{in}]$ to obtain a first solution μ_1 (with initial conditions $\mu_1(a = 0.0001)$ and $\frac{d\mu_1}{da}(a = 0.0001)$). Then, we solve eq. (20) with the Hubble factor in eq. (14) for $a \in [a_{in}, 1]$ to obtain a second solution $\mu_2(a)$ with initial conditions at $a = a_{in}$, with matching of the first solution μ_1 at $a = a_{in}$ ($\mu_2(a = a_{in}) = \mu_1(a = a_{in})$ and $\frac{d\mu_2}{da}(a = a_{in}) = \frac{d\mu_1}{da}(a = a_{in})$).

We first compute the potential term in eq. (19) for different free-parameter choices in order to determine which one has the biggest impact on the amplitude. We note that Ω_{G0} affects the amplitude of PGW only via a_{in} , as the Hubble factor (and, consequently, eq. (20)) do not explicitly depends on Ω_{G0} . The parameter Ω_{m0} is chosen in the 2- σ region shown in figure 2, while Ω_{i0} is chosen to lie on the $\Omega_{dm0} + \Omega_{G0} > 0$ region. Figure 3 shows the potential vs. scale factor for different parameter choices. The one parameter with a noticeable impact on the potential is Ω_{m0} , while the rest of the free parameters leave the potential unchanged up to eye view.

The PGW amplitude depends on Ω_{m0} as expected (figure 4). The larger parameter Ω_{m0} the larger the resulting PGW amplitude. Also, for different wave numbers k , the amplification of the same free parameters varies as well. In the next section, we compute the PGW power spectrum, related to the amplitude, as a function of Ω_{m0} .

IV. POWER SPECTRUM

In this section, we consider the best-fit value for the Hubble factor $H_0 = 70 \text{ km}/(\text{Mpc s}) \simeq 2.27 \times 10^{-18} \text{ s}^{-1}$ obtained in [26], as we use units for the frequency and wave number. The wave number k is not a physical quantity (it is defined a comoving quantity), while the corresponding physical frequency is defined as $\omega(a) = k/a$. Given that $a_0 = 1$, we use that the frequency of the PGW observed today corresponds to the wavenumber $k = \omega$. The PGW amplitude depends on their wave number and the amplification regime experienced through the expansion of the universe.

We assume a typical slow-roll de Sitter inflation with $H_1 = 10^{35} \text{ s}^{-1}$, at the inflation-radiation transition η_1 . It is straightforward that

$$a_1 = 0.0001 (H(a_2)/H_1)^{1/2},$$

with $H(a_2)$ being the Hubble factor at the beginning of the dust/IBEG era, which depends

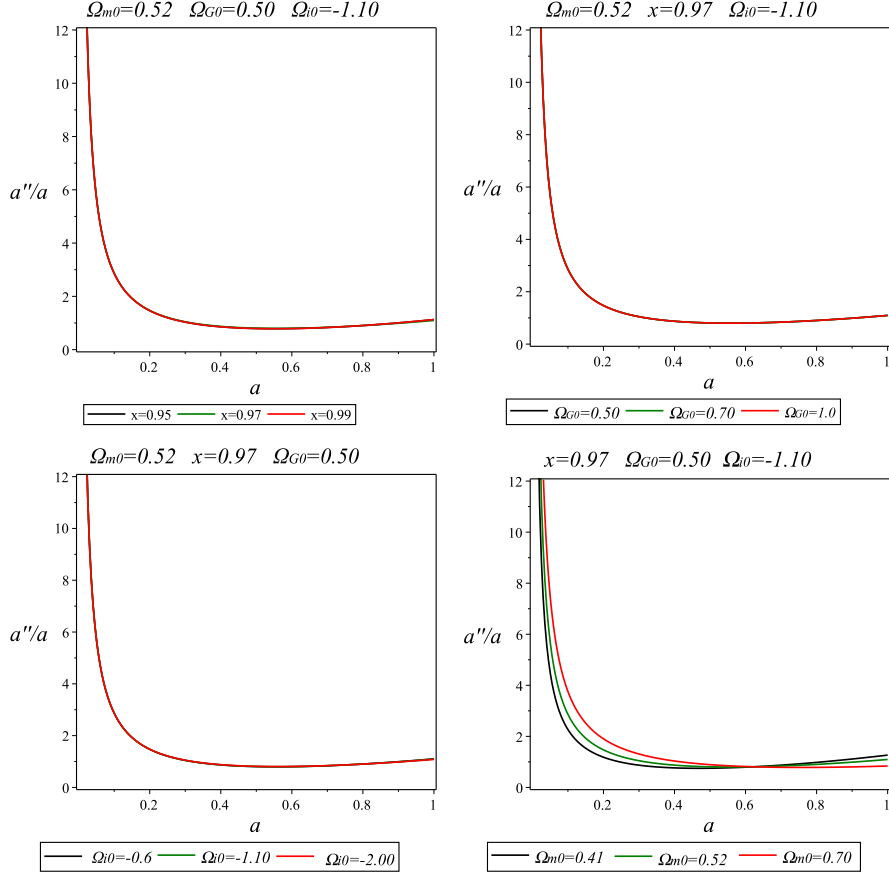


FIG. 3: Potential a''/a vs. scale factor a , with each plot varying x , Ω_{G0} , Ω_{i0} and Ω_{m0} , and fixing the other parameters. The one parameter with a noticeable impact on the potential is Ω_{m0} , as the rest of the free parameters leave the potential unchanged up to eye view.

on the IBEG-model free parameters as well. In all cases, the bound is of order $K_1^2 = a_1 H_1 \sim 10^{11} \text{s}^{-1}$. As stated in section II, waves with $k \gg K_1 \sim 10^{11} \text{s}^{-1}$ did not experience any adiabatic amplification and have an amplitude several orders of magnitude smaller at present than at the instant they were generated. Consequently, we can assume that those waves do not contribute to the PGW power spectrum.

PGW with wave number $k^2 \ll K_1$ but $k^2 \gg \frac{a''}{a}(a = a_2)$ evolve as free waves, after a first amplification regime during inflation, and are not affected by the late-universe dynamics. For $a = a_2 = 0.0001$, we define this bound as $K_2^2 = \frac{a''}{a}(a_2)$, which also depends on free parameters through $H(a_2)$ and $\frac{dH(a_2)}{da}$. The PGW amplitude in this regime is proportional to

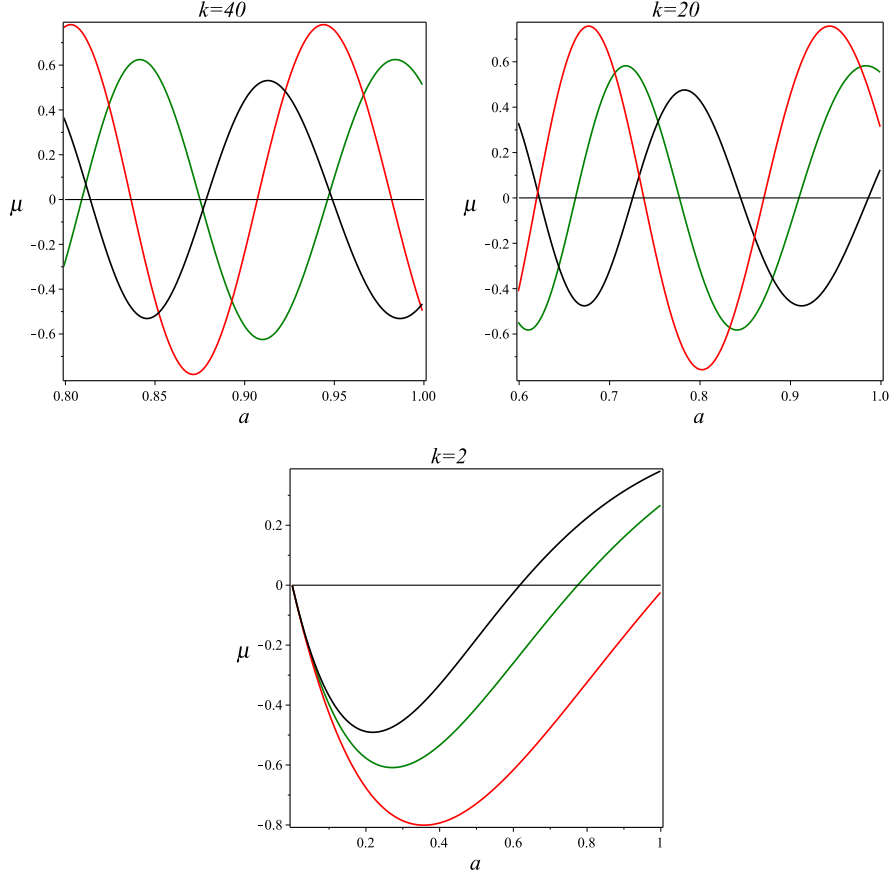


FIG. 4: Evolution of PGW amplitude for the IBEG model from the beginning of dust $a = 0.0001$ until today $a = 1$ era with $x = 0.97$, $\Omega_{G0} = 0.5$, and $\Omega_{i0} = -1.10$ for different wave number choices: $k = 40$, $k = 20$, and $k = 2$. The black line represents the evolution with $\Omega_{m0} = 0.41$, the green line represents $\Omega_{m0} = 0.52$, and the red line represents $\Omega_{m0} = 0.70$

$$\frac{C_D}{C_I} \sim \begin{cases} 1 & (k \gg K_1), \\ k^{-2} & (K_1 \gg k \gg K_2), \end{cases}$$

and they are considered in the power spectrum.

PGW with $k \ll K_2$, undergo an amplification during inflation and a second one in the dust/IBEG eras. On the other hand, the perturbations whose wave number is $k \ll (a''/a)(a = 1) = K_0^2$ have wavelengths larger than the Hubble radius of the universe, i.e. on the whole history of the universe, they have not completed a single period of oscillation. Those perturbations cannot be considered as physical waves. This puts a lower bound on the wave number for the PGW spectrum, K_0 , that also depends on the free parameters.

The waves with $K_2 \ll k \ll K_1$ have the same power spectrum as in [23]

$$P(k) = \frac{\hbar}{4\pi^2 c^3} a_1^4 H_1^4 k^{-1}, \quad (21)$$

where the initial perturbations on the inflationary field are Gaussian, thus, $C_I \propto k^2$ [9].

The power spectrum of the waves with $K_0 \ll k \ll K_2$ is obtained by numerically computing $\mu(a)$ for each k as in the previous section. We consider, then,

$$P(k) = \frac{\hbar}{4\pi^2 c^3} k^3 |\mu_{rms}|^2 \quad (22)$$

where $|\mu_{rms}|$ is the root mean square of the PGW as

$$|\mu_{rms}|^2 = \frac{2}{(1 - a_p)} \int_{a_p}^1 \mu(a)^2 da \quad (23)$$

where a_p corresponds to the scale factor for which the corresponding $k\eta(a_p) = 2\pi$, i.e., the scale factor at the start of the last oscillation of the PGW.

Figure 5 shows $\log_{10}(P(k))$ vs $\log_{10}(k)$ for the IBEG-model PGW, for $x = 0.97$, $\Omega_{G0} = 0.5$, $\Omega_{i0} = -1.10$, and Ω_{m0} choices. The power spectrum dependence on Ω_{m0} is expressed in the slope of the line for $k < K_2 \approx 10^{-16}$ and also on the bounds K_1 , K_2 , K_0 . The rest of free parameters do not affect significantly the power-spectrum slope or K_1 , K_2 , K_0 .

Another relevant definition is the fraction of energy density per frequency [29]

$$\Omega_{gw}(k, a) = \frac{3}{8\pi G H^2} \frac{d\rho_{gw}}{d(\ln k)} = \frac{4}{3\pi a^2 H^2} \frac{H_1}{M_{pl}^2} |T'|^2, \quad (24)$$

where T' is a transfer function related to $(\mu/a)'$ for waves with $k < K_2$ during the IBEG stage of expansion, and ρ_g is the energy density of the PGW obtained from tensor first order perturbation theory as

$$\rho_{gw} = \frac{1}{32\pi G a^2} \langle h_{ij}' h^{ij'} \rangle. \quad (25)$$

The observational bounds suggest that present day ($a = 1$) $\Omega_{gw} h^2 < 10^{-15}$ for frequencies $k \sim 10^{-17}$ with $h = H_0/(100 \text{ km}/(\text{Mpc s}))$ [30]. Although these bounds are strongly related to inflation and reheating parameters of the cosmological model, the late-accelerated expansion model should be taken into account, as for low frequencies $|(\mu/a)'|^2$ depends on H . In our case, assuming the above free-parameter choices ($x = 0.97$, $\Omega_{G0} = 0.5$, and $\Omega_{i0} = -1.10$) with $h = 0.7$, present-day Ω_{gw} at several wave numbers of order $k = 10^{-17}$ were computed

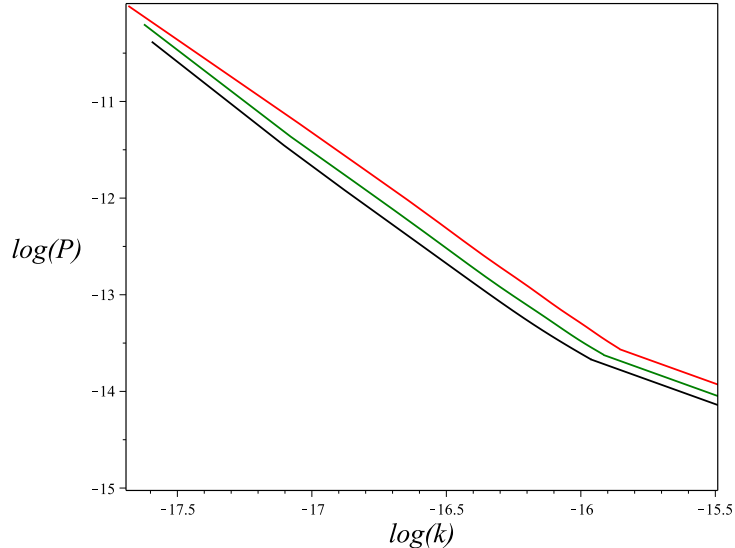


FIG. 5: IBEG-model power spectrum P with $x = 0.97$, $\Omega_{G0} = 0.5$, and $\Omega_{i0} = -1.10$. The black line represents $\Omega_{m0} = 0.41$, the green line $\Omega_{m0} = 0.52$, and the red line $\Omega_{m0} = 0.70$. P and the frequency k are expressed in erg s/cm^3 and s^{-1} , respectively.

for some values of Ω_{m0} : $\Omega_{m0} = 0.41$, $\Omega_{m0} = 0.52$, $\Omega_{m0} = 0.70$, and $\Omega_{m0} = 0.75$. The results are shown in figure 6. The last Ω_{m0} value is out of the $2\text{-}\sigma$ region of figure 2, but close enough as not to be excluded beforehand.

We note that the present-day Ω_{gw} bound is heavily dependent on the inflation model considered, and it is not a PGW prediction per se, but an order of magnitude estimate. It would be erroneous to strictly bound parameters of the late-acceleration model considered (IBEG model in this work) from it. However, it is safe to conclude that the late accelerated-model parameters have a non-negligible impact on Ω_{gw} as do inflation parameters (we have used $H_1 = 10^{35} \text{ s}^{-1}$). In our model, only parameter Ω_{m0} has a noticeable impact on present-day Ω_{gw} , and, the higher Ω_{m0} is, the higher Ω_{gw} . At wave number $k = 10^{-17}$, Ω_{gw} reaches the highest value for $\Omega_{m0} = 0.75$ (with Ω_{gw} for $\Omega_{m0} = 0.70$ slightly lower), but an order of magnitude smaller than the observational limit. Choosing $H_1 = 10^{36} \text{ s}^{-1}$ would lead to Ω_{gw} for both $\Omega_{m0} = 0.75$ and $\Omega_{m0} = 0.70$ reaching the observational limit, while the smaller Ω_{m0} values would be still one or two order of magnitude under it.

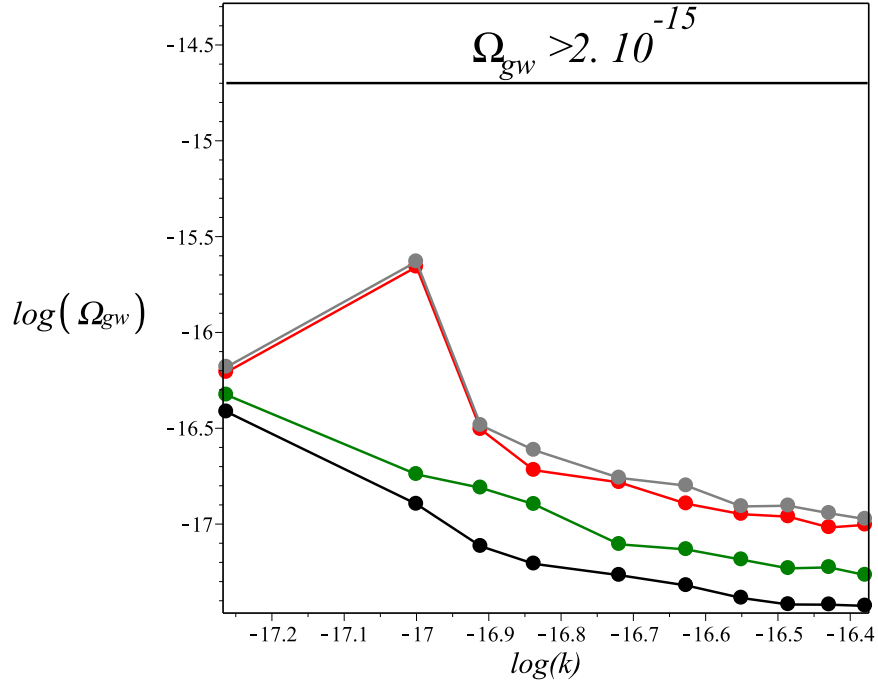


FIG. 6: $\log(\Omega_{gw}(a = 1))$ computed at different discrete choices of wave number ($k \sim 10^{-17}$) for $H_1 = 10^{35} \text{ s}^{-1}$, $x = 0.97$, $\Omega_{G0} = 0.5$, and $\Omega_{i0} = -1.10$, Hubble parameter $h = 0.7$, and different values of Ω_{m0} parameter (the black line represents $\Omega_{m0} = 0.41$, the green $\Omega_{m0} = 0.52$, the red $\Omega_{m0} = 0.70$, and the grey $\Omega_{m0} = 0.75$). The top straight line separates the region fulfilling the observational bound $\Omega_{gw}(a = 1) < 2 \cdot 10^{-15}$ from the region excluded by observations.

V. CONCLUSIONS

PGWs are second-order tensorial wave-like solutions to the cosmological Einstein equations that are generated and amplified by the universe dynamics. Inflation and early phase transitions are crucial to the amplification process, but the late accelerated expansion has also an important contribution to the low-frequency wave evolution [21, 23].

In particular, the IBEG model is applied for a flat late-acceleration expansion with a detailed microscopical description. The IBEG model has four free parameters: Ω_{G0} , Ω_{m0} , related to the dark-energy, rest-mass energy density and the dark-matter term scaling as a mass term, respectively; Ω_{i0} , the self-interaction intensity; x , the energy exchange rate. Other parameters of the model are the Hubble constant H_0 and the baryonic matter parameter Ω_{b0} . The free parameters can be bounded by observational data [26].

The PGW amplitude evolution in the IBEG model depends on the free parameters

through the Hubble factor $H(a)$ in eq. 14 and its derivative dH/da . When considering different values for the free parameters we conclude that only parameter Ω_{m0} has a noticeable impact. The higher Ω_{m0} , the larger the PGW amplitude for constant wave number. The PGW power spectrum depends consequently on the parameter Ω_{m0} . Additionally, the fraction of energy density per frequency $\Omega_{gw}(k, a)$ has a non trivial dependency on parameter Ω_{m0} at low frequencies. We also derived the model's PGW power, which is consistent with observational bounds from below, similarly to other models.

Acknowledgements

The authors acknowledge support from the Dirección General de Asuntos del Personal Académico, at the Universidad Nacional Autónoma de México, through Project IN117020.

Data access statement

The authors declare that the data supporting the findings of this study are available within the article.

References

- [1] A. Einstein, Preuss. Akad. Wiss. Berlin, Sitzber, 688 (1916).
- [2] R. A. Hulse and J. H. Taylor, *Astrophys. J. Lett.* 195, L51 (1975).
- [3] B. P. Abbott et al. [LIGO Scientific and Virgo Collaborations], *Phys. Rev. Lett.* 116, 061102 (2016).
- [4] Schutz, B. F., *Nature*, 323, 310 (1986).
- [5] Abbott, T. D. *et al.*, The LIGO Scientific Collaboration *Nature* **551** 85-88 (2017).
- [6] Ade P A, Aghanim N, Arnaud M, Ashdown M, Aumont J, Baccigalupi C, Banday A, Barreiro R, Bartlett J, Bartolo N *et al.* *Astronomy & Astrophysics* **594** A13 (2016).
- [7] Riess A G, Macri L M, Hoffmann S L, Scolnic D, Casertano S, Filippenko A V, Tucker B E, Reid M J, Jones D O, Silverman J M *et al.* *The Astrophysical Journal* **826** 56 (2016).
- [8] E. Lifshitz, *J. Phys. USSR* **10**, 116 (1946).
- [9] L. P. Grishchuk, *Zh. Eksp. Teor. Fiz.* **67**, 825 (1975) [*Sov. Phys. JETP* 40, 409 (1975)].
- [10] B. P. Abbott et al. [LIGO Scientific and Virgo Collaborations], *Phys. Rev. Lett.* 118, 121101 (2017).

- [11] <https://www.elisascience.org/>
- [12] U. Seljak and M. Zaldarriaga, *Physical Review Letters*, **78**, 2054 (1997). D. N. Spergel and M. Zaldarriaga, *Physical Review Letters*, **79**, 2180 (1997)
- [13] Cheng Cheng, Qing-Guo Huang, arXiv:1403.5463.
- [14] Copeland E J, Sami M and Tsujikawa S 2006 *International Journal of Modern Physics D* **15** 1753-1935
- [15] Wang B, Abdalla E, Atrio-Barandela F and Pavón D 2016 *Reports on Progress in Physics* **79** 096901
- [16] J. D. Barrow and T. Clifton, *Phys. Rev. D* **73** 103520 (2006).
- [17] M. Shahalam et al., *Eur. Phys. J. C* **75** 395 (2015).
- [18] S. Ray et al., *Int. J. Theor. Phys.* **50** 939-951, (2011).
- [19] I. G. Dymnikova and M. Yu. Khlopov, *Mod. Phys. Lett. A* **15**, 2305-2314 (2000).
- [20] I. G. Dymnikova and M. Yu. Khlopov, *Eur. Phys. J. C* **V. 20**, PP. 139-146 (2001).
- [21] G. Izquierdo and D. Pavón, *Physical Review D* **70** 084034 (2004).
- [22] T. Sasaki and H. Suzuki, *Progress of Theoretical and Experimental Physics*, Volume, 11, 113E03 (2018).
- [23] M. L. Sosa-Almazan and G. Izquierdo, *General Relativity and Gravitation* **46** 1759 (2014).
- [24] G. Izquierdo and J. Besprosvany, *Classical and Quantum Gravity*, **27** 065012 (2010).
- [25] J. Besprosvany and G. Izquierdo, *Classical and Quantum Gravity*, **32** 055015 (2015).
- [26] H. E. Lucatero-Villaseñor, G. Izquierdo and J. Besprosvany, *General Relativity and Gravitation*, **50**, 151 (2018).
- [27] L. P. Grishchuk, *Class. Quantum Grav.* **10**, 2449 (1993).
- [28] M. Yu. Khlopov, B. A. Malomed and Ya. B. Zeldovich, *Mon. Not. Roy. astr. Soc.* **215**, 575-589 (1985).
- [29] Y. Watanabe and E. Komatsu, *Physical Review D* **73** 123515 (2006).
- [30] M. C. Guzzetti, N. Bartolo, M. Liguori, and S. Matarrese, *Rivista del Nuovo Cimento*, Vol. 39, Issue 9, 399-495 (2016).
- [31] For a particle Markoffian creation process the number of particles evolves as $N \propto V^x$ where V is the volume considered and x is a parameter as the distribution of future states of it does not depend on previous states. Typical dispersion processes and fluid interactions lead to evolution laws of this type in various physical setups [25].